# Functional Characterization of Two Isoforms of GPR39 Gene

A Dissertation Submitted to

the Graduate School of Life and Environmental Sciences,

the University of Tsukuba

in Partial Fulfillment of the Requirements

for the Degree of Doctor of Philosophy in Biotechnology

(Doctoral Program in Life Sciences and Bioengineering)

Shin-ichiro YASUDA

# ABBREVIATIONS

| | |
|---|---|
| AC | adenylate cyclase |
| AcOH | acetic acid |
| AMP | adenosine monophosphate |
| BRET | bioluminescence resonance energy transfer |
| BSA | bovine serum albumin |
| cAMP | cyclic AMP |
| cDNA | complementary DNA |
| CE | cation exchange |
| CNS | central nervous system |
| cpm | count pre minute |
| CRE | cAMP responsive element |
| Da | Dalton |
| DMEM | Dulbecco's modified eagle medium |
| DNA | deoxyribonucleic acid |
| EDTA | ethylenediaminetetraacetic acid |
| FBS | fetal bovine serum |

| | |
|---|---|
| GFP | green fluorescent protein |
| GI tract | gastrointestinal tract |
| GPCR | G protein-coupled receptor |
| G protein | GTP-binding protein |
| GTP | guanosine triphosphate |
| HPLC | high performance liquid chromatography |
| ICP-MS | inductively coupled plasma-MS |
| Luc | luciferase |
| MAP kinase | mitogen activated protein kinase |
| MM | multi-mode |
| mRNA | messenger RNA |
| MS | mass spectrometry |
| NTS | neurotensin |
| PBS | phosphate buffered saline |
| PCR | polymerase chain reaction |
| PKA | protein kinase A |
| PLC | phospholipase C |
| ppb | parts per billion |

| | |
|---|---|
| PTx | pertussis toxin |
| RhoGEF | Rho guanine nucleotide exchanging factor |
| RLuc | *Renilla* luciferase |
| RNA | ribonucleic acid |
| rpm | revolution per minute |
| RT-PCR | reverse transcription-PCR |
| SDS | sodium dodecyl sulphate |
| S.E. | standard error |
| SRE | serum responsive element |
| TFA | trifluoroacetic acid |
| YFP | yellow fluorescent protein |

# CONTENTS

CHAPTER Ⅰ. PREFACE ..... 8

CHAPTER Ⅱ. ISOLATION OF $Zn^{2+}$ AS AN ENDOGENOUS AGONIST OF GPR39-1a FROM FETAL BOVINE SERUM ..... 12

1. Summary ..... 12

2. Introduction ..... 13

3. Materials and Methods ..... 15

3.1. Cloning of GPR39-1a genes ..... 15

3.2. Stable expression of hGPR39-1a ..... 15

3.3. Conditioning of peptide fraction from fetal bovine serum (FBS) ..... 16

3.4. Fractionation with cation-exchange (CE) column. ..... 16

3.5. Fractionation with multi-mode (MM) column ..... 17

3.6. Calcium mobilization assays ..... 18

3.7. Determination of metal concentrations ..... 18

3.8. Transient expressions of GPR39-1a genes ..... 19

4. Results ..... 20

4.1. Finding of active fraction by cation-exchange HPLC ..... 20

4.2. Purification of the active fraction ..... 20

4.3. Identification of endogenous agonist of GPR39-1a as $Zn^{2+}$ ion ..... 21

4.4. Responsiveness of GPR39-1a against divalent metal ions ..... 22

4.5. Characterization of signaling pathway of GPR39-1a ..... 22

5. Discussion ..... 24

6. Figures and Tables ..... 27

CHAPTER Ⅲ. GPR39-1b INTERACTS WITH NEUROTENSIN RECEPTOR NTSR1 AND MODIFIES ITS FUNCTION ..... 34

1. Summary ..... 34

2. Introduction ..... 36

3. Materials and Methods ..... 38

3.1. Cloning of genes ..... 38

3.2. Calcium mobilization assays ..... 38

3.3. CRE-luciferase reporter assays ..... 39

3.4. $BRET^2$ assays ..... 40

4. Results ..... 42

4.1. Calcium mobilization assays in the cells transfected with GPR39-1b ..... 42

4.2. $BRET^2$ assays to evaluate the homodimerization and heterodimerization across the

isoforms of GPR39 gene..... 42

4.3. BRET$^2$ assays to explore the heterodimeric counterpart of GPR39-1b..... 43

4.4. CRE-Luc assays to evaluate the functional effects of heterodimerization on the signaling activity of NTSR1..... 45

5. Discussion.....46

6. Figures and Tables .....49

CHAPTER Ⅳ. CONCLUDING REMARKS..... 54

CHAPTER Ⅴ. ACKNOWLEDGEMENTS ..... 54

CHAPTER Ⅵ. REFERENCES..... 57

# CHAPTER Ⅰ. PREFACE

G protein-coupled receptor (GPCR) is one of the largest superfamily of transmembrane proteins. Based on the similarities in amino acid sequence, they are classified as 6 groups, rhodopsin like (class A), secretin (class B), metabotropic glutamate (class C), fungal mating pheromone (class D), cAMP (class E) and frizzled/smoothened (class F) receptors. Commonly, GPCRs have 7 transmembrane domains and work as receptors that transduce extracellular signals into intracellular signals.

Generally, GPCRs are residing in the plasma membrane and form complexes with 3 subunits of intracellular G proteins called Gα, Gβ, and Gγ. When a GPCR senses the extracellular signals, it makes conformational change so that the complex is disassembled. The Gα subunits dissociated from the complexes act on the effectors that transduce intracellular signals. The signals triggered by GPCR depend on the types of Gα subunit involved. In mammals, 16 types of Gα subunits are known, and most of them are classified as four groups, $G_{q/11}\alpha$, $G_{12/13}\alpha$, $G_s\alpha$, and $G_{i/o}\alpha$. $G_{q/11}\alpha$ activates phospholipase C (PLC) to mobilize intracellular calcium. $G_{12/13}\alpha$ activates various kinds of MAP kinases thorough the activation of RhoGEF. $G_s\alpha$ activates adenylate cyclase (AC) to increase intracellular cyclic AMP (cAMP), while $G_{i/o}\alpha$ inhibits AC to reduce cAMP.

Extracellular molecules that bind to GPCRs and activate them are called ligands. Ligands include many types of molecules such as proteins, peptides, nucleotides, lipids, amine derivatives, and so on. Most of them are hormones that regulate physiological functions and play important roles in central nervous system (CNS), immune system, metabolism, circulation, and so forth. Also, it is known that many GPCR signals are known to be involved in incidence or progression of common diseases. Exogenously-administered molecules that modify these signals can be therapeutic drugs and GPCR is thought to be one of the most successful molecular classes for drug target. Indeed, 36% of marketed drugs are targeted on GPCRs (1). Therefore, GPCRs have been subjects of considerable research interest by pharmaceutical companies and academic institutes.

Up to this time, there still remain many GPCRs whose ligands and functions are unknown. They are called “orphan” GPCRs. Exploration of the endogenous ligands of orphan GPCRs are called deorphanization. From 1990s to 2000s, many deorphanizations were demonstrated and opened new frontier of physiology. For instance, in 1999, Kangawa and his colleagues found ghrelin as a ligand of the growth hormone secretagogue receptor (GHSR) (2). Their findings gave a new understanding on appetite control of mammals.

In the present study, the focus is put on G protein-coupled receptor 39 (GPR39), an orphan GPCR. GPR39 is classified as a member of the ghrelin receptor family in class A

GPCRs, based on its amino acid sequence (3). Due to its expression patterns and the phenotypes of genetically engineered models, GPR39 is thought to have crucial roles in metabolism and nutrient intake.

The translational product of the GPR39 gene is known to have two isoforms, GPR39-1a and GPR39-1b (4). As shown in Fig. 1, GPR39-1a is a full-length 7-transmembrane receptor, while GPR39-1b is a 5-transmembrane protein. Assuming from the structure, GPR39-1a may retain functions as a GPCR. On the other hand, it is unpredictable whether if GPR39-1b has functions as GPCRs, since it lacks TMⅥ, Ⅶ, and C-terminal domains that are crucial for functions of GPCRs.

The purpose of the present study is to clarify the molecular functions of these two isoforms in order to provide a clue to understand the physiological significance of the GPR39 gene. In the Chapter 2, the natural ligands of GPR39-1a were explored from fetal bovine serum (FBS) using liquid chromatography and mass spectrometry. In the Chapter 3, the molecular function of GPR39-1b was explored using Bioluminescence Resonance Energy Transfer (BRET) system, noticing interaction between GPR39-1b and other GPCRs.

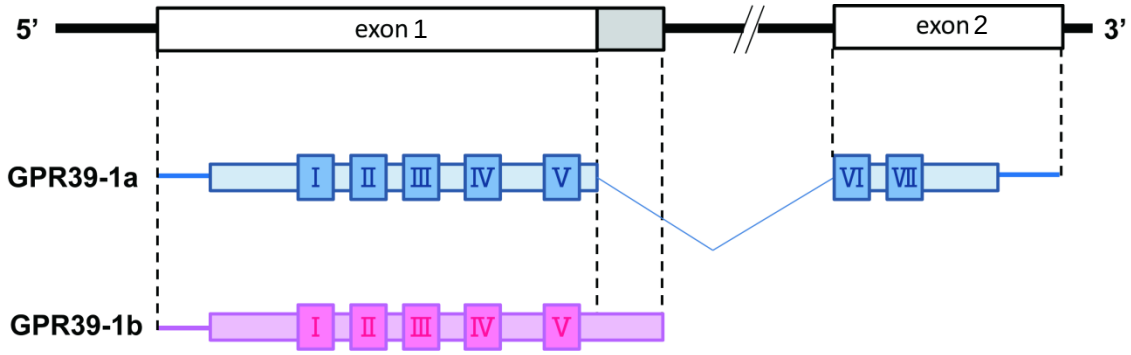


Fig. 1 Schematic illustration of the gene structure of GPR39-1a and GPR39-1b.
Each transcript is put with the 5’-terminus on the left and 3’-terminus on the right. Colored thick bars and boxes correspond to the coding regions and transmembrane domains respectively. The Roman numeral on each box refers to its number from the C-terminus of each protein product. Dotted lines indicate the regions retaining identical sequences. mRNA for GPR39-1a consists of two exons and the product of it contains 7 transmembrane domains. Meanwhile, the mRNA for GPR39-1b consists of single exon and the product of it contains 5 transmenbrane domains.

# CHAPTER Ⅱ. ISOLATION OF $Zn^{2+}$ AS AN ENDOGENOUS AGONIST OF GPR39-1a FROM FETAL BOVINE SERUM

## 1. Summary

In this chapter, determination of the natural agonists of GPR39-1a from fetal bovine serum (FBS) is attempted. FBS was conditioned to extract peptides and fractionated by two types of HPLC. The activity of each fraction was monitored by intracellular calcium mobilization. Then the purified active ingredient was analyzed by inductively coupled plasma mass spectrometry (ICP-MS). In this fashion, $Zn^{2+}$ ion was identified as an agonist of GPR39-1a, though no peptidergic molecules were found. The calcium-mobilizing activity of $Zn^{2+}$ was not abolished by pertussis toxin, but was by a phospholipase C (PLC) inhibitor, U73122, indicating that the activity of GPR39-1a is mediated through the $G_q$α-PLC pathway. In addition, $Zn^{2+}$ also activated mouse and rat GPR39-1a, showing that the function of GPR39-1a as a $Zn^{2+}$ receptor is conserved across species. This study is the first exploration of GPR39-1a agonists in FBS, and indicates that GPR39-1a functions as a $G_q$-coupled $Zn^{2+}$-sensing receptor.

## 2. Introduction

GPR39-1a, a full length product of the GPR39 gene, is one of the rhodopsin type G protein-coupled receptors (GPCRs). It is classified as a member of the ghrelin receptor family based on similarities in amino acid sequence (3). This family consists of ghrelin, motilin, and neurotensin receptors (3). Because each of these family members has important functions, especially in the gastrointestinal (GI) tract, it is expected that GPR39-1a may similarly play roles in the digestive system. Nevertheless, the function of GPR39-1a was completely unknown until recently, because its endogenous ligand had remained unidentified following its first cloning in 1997 (5).

In 2004, Holst *et al.* (3) reported that GPR39-1a is constitutive active in both $IP_3$ accumulation and serum responsive element (SRE) activation. More recently, Zhang *et al*. identified a novel peptidergic hormone, obestatin, from rat stomach (6). This preproghrelin-derived 23-amino-acid peptide reportedly suppresses food intake, and acts as an endogenous ligand of GPR39-1a. The concentration of obestatin in serum is extremely low and below efficacious levels, though it is present in sufficient amounts to activate GPR39-1a in the stomach, the organ that produces it (6). Since GPR39-1a is expressed not only in the GI tract but in many other peripheral and central tissues (5, 7), it would not be surprising if other endogenous ligands for it existed. Moreover, several reports that obestatin dose not affect

GPR39-1a have very recently been published (8 - 11).

I therefore searched for non-obestatin ligands from serum extracts. Considering both availability and reproducibility, commercialized fetal bovine serum (FBS) was chosen as a starting material. Because the endogenous ligands of GPR39-1a are expected to be peptidergic, the isolation procedure was based on a method for extraction of peptides (12) with some modifications to handle serum (13).

# 3. Materials and Methods

## 3.1. Cloning of GPR39-1a genes

Full-length cDNAs of human and mouse GPR39-1a (hGPR39-1a and mGPR39-1a, respectively) were obtained by ligations of the two exons amplified by PCR from genomic DNAs, while one of rat GPR39-1a (rGPR39-1a) was obtained by reverse transcriptase-PCR (RT-PCR) from first-strand cDNA of rat liver. The primers for hGPR39-1a were designed based on the reported mRNA sequence (accession number: NM_001508 in National Center for Biotechnology Information; http://www.ncbi.nlm.nih.gov/), while those for mGPR39-1a and rGPR39-1a were designed based on the sequences predicted by homology searches with hGPR39-1a against mouse or rat genomic DNAs. Each amplified DNA was ligated into pCDNA3.1 vector (Invitrogen, Grand Island, NY) and fused with the signal peptide MSALLILALVGAAVA of preprotrypsin (14) and a FLAG-tag in the N-terminal.

## 3.2. Stable expression of hGPR39-1a

The expression vector signal-FLAG-hGPR39-1a-pCDNA3.1 was transfected into CHO-K1 cells. Stably expressing cells were selected in 600 mg/L Geneticin (Invitrogen) and cloned by the limiting dilution method. Expression of hGPR39-1a was confirmed by RT-PCR and western immunoblot with monoclonal ANTI-FLAG M2 antibody (Sigma-Aldrich, St.

Louis, MO). One of the clones, HC48, was chosen for use in the calcium mobilization assays because of its high expression, reactivity, and growth rate.

## 3.3. Conditioning of peptide fraction from fetal bovine serum (FBS)

Fetal bovine serum (Hyclone, South Logan, UT) was deproteinized by 1 M acetic acid (AcOH) and 40% ethanol, followed by centrifugal separation at a rate of rotation of 5,000 rpm for 30 min. The supernatant was filtered with a Minisette Omega 10K 10 KDa cut-off ultrafilter (Filtron Technology Corp., Northborough, MA). The filtrate was loaded onto a Mega Bond Elut$^{Flash}$ C18 reverse-phase column (Varinan inc., Palo Alto, CA) pre-equilibrated in 10% acetonitrile and 0.1% trifluoroacetic acid (TFA). The absorbate was eluted in 60% acetonitrile containing 0.1% TFA after washing with 10% acetonitrile containing 0.1% TFA. The eluate was evaporated, and the residual material was redissolved in 1 M AcOH. This portion was designated the peptide fraction and subjected to ligand searches.

## 3.4. Fractionation with cation-exchange (CE) column.

The peptide fraction from FBS was separated by high performance liquid chromatography (HPLC) on the AKTA explorer 10S system (GE Healthcare, Piscataway, NJ)

with a Mini S PE 4.6/50 cation-exchange (CE) column (GE Healthcare). A gradient was provided at a flow rate of 500 μL/min by changing the mixing ratio of two eluents: A, 1M AcOH and B, 1M AcOH containing 1M NaCl. The proportion of B was initially 0% and increased to 50% over 16.6 min. The activity of each fraction was monitored by calcium mobilization in HC48, a cell line stably expressing hGPR39-1a. In this assay, an aliquot of each fraction equivalent to 10 mL serum was evaporated, redissolved and added to the cells suspended in a total volume of 50 μL buffer. Each of the components was thus condensed by 200-fold of the yield.

### 3.5. Fractionation with multi-mode (MM) column

The active fraction was further fractionated by HPLC on an AKTA explorer 10S with a TSKgel VMpak-25 multi-mode (MM) column (Tosoh, Tokyo, Japan), which has both reverse-phase and cation-exchange characteristics. A gradient was provided at a flow rate of 500 μL/min by changing the mixing ratio of two eluents: A, 10% (v/v) acetonitrile containing 9 mM ammonium acetate - NaOH (pH 9.0) and B, 80% (v/v) acetonitrile containing 0.05% TFA. The proportion of B was initially 20% and increased to 91.4% in 33.2 min. The activity of each fraction was monitored by calcium mobilization in HC48. The tested amount of an aliquot in the assay was the same as for CE.

## 3.6. Calcium mobilization assays

Cells were grown in DMEM/F12 (Invitrogen) supplemented with 10% FBS. After depletion of serum for 5 hours, cells were harvested by 0.025% Trypsin-EDTA (Invitrogen) and loaded with 4 μM Fluo-3AM (Molecular Probes, Inc., Eugene, OR) for 1 hour in assay buffer (Hank's balanced salt solution supplemented with 10 mM HEPES, 2.5 mM probenecid, and 0.1% BSA). After loading, cells were washed twice with assay buffer and plated at $2.0 \times 10^4$ cells/well in half-area clear-bottom black plates (Coring Corstar Co., Cambridge, MA). Intracellular calcium ion was detected by monitoring of fluorescence of 540 nm with excitation at 480 nm on the Functional Drug Screening System 6000 (Hamamatsu Photonics KK, Hamamatsu, Japan). The fluorescence intensity of each sample was recorded every 1.095 seconds for about two minutes, with the tested samples added 10.95 seconds after the beginning of measurements. For each tested sample, I calculated the maximum fluorescence ratio over the baseline during two minutes, and considered it the intensity of calcium response. To detect GPR39-1a-specific activity, the intensity of each fraction was compared with that measured with the host cells, CHO-K1, in the same fashion.

## 3.7. Determination of metal concentrations

An aliquot of the purified fraction equivalent to 200 mL FBS was evaporated and

redissolved in 10 mL of 1% nitric acid. I examined the solution by inductively coupled plasma mass spectrometry (ICP-MS) to determine the concentrations of Zn, Cu, Mg, Fe, Mn, Cr, and Se. The concentration of each metal was calculated from the intensity of each m/z value with the calibration curve determined using the ICP multi-element standard solution IV (Merck KGaA, Darmstadt, Germany). These measurements were performed on the ICPM-8500 system (Shimadzu, Kyoto, Japan).

### 3.8. Transient expressions of GPR39-1a genes

CHO-K1 cells were plated on 100 mm-diameter culture dishes at $1.5 \times 10^6$ cells/dishes on the day before transfection. Transfection was performed by the lipofection method using Lipofectamine2000 (Invitrogen). The amount of transfected vector was 12 μg per one dish. The cells were subcultured the following day, and used for calcium assays on the third day after transfection.

# 4. Results

## 4.1. Finding of active fraction by cation-exchange HPLC

First, the peptide fraction conditioned from FBS was fractionated by cation-exchange (CE) HPLC. An aliquot of each fraction was subjected to calcium mobilization assay with HC48, the cell line stably expressing human GPR39-1a (hGPR39-1a), and CHO-K1, the host cell. Strong activities specific to HC48 were found in the fractions eluted from 17.5 to 17.9 min (total flow volume of 8.7 mL to 8.9 mL) (Fig. 2a, b). This finding indicates that GPR39-1a-activating components are contained in FBS and positively charged. The active fractions obtained by CE HPLC were pooled and processed by further fractionation to enable purification.

## 4.2. Purification of the active fraction

I examined several types of HPLC for use in the next step of fractionation, and finally chose a multi-mode (MM) column with both reverse-phase and cation-exchange properties. With this type of HPLC, activities were clearly detected in the fractions eluted around 40.8 min (total flow volume of 20.4 mL) (Fig. 3a, b), which corresponded to the inflection point on the conductivity curve. This finding suggests that the active components were absorbed in the column in the starting condition, and were eluted by the acute change in

conductivity. In the calcium mobilization assays, these fractions exhibited quick, transient increases in intracellular calcium in HC48 alone (Fig. 3c), indicating the presence of specific agonists of GPR39-1a coupling to $G_q\alpha$ or $G_i\alpha$. Presuming these fractions to be purified, I pooled and processed them for mass spectroscopy (MS) measurements.

## 4.3. Identification of endogenous agonist of GPR39-1a as $Zn^{2+}$ ion

Because the active constituent was expected to be a peptidergic molecule, MS and MS/MS measurements on the purified fraction were performed. However, no m/z values assignable to peptides were detected. This finding indicates that the active molecule is not a peptide, or that its concentration was below the limit of detection. Next, I considered the possibility of metal ions. Indeed, Holst *et al*. had previously shown that $Zn^{2+}$ ion enhances $IP_3$ accumulation in GPR39-1a-expressing cells (1, 8). To examine this possibility, I re-assayed the purified fraction mixed with EDTA. The activity was eliminated by 300 nM of EDTA (Fig. 3c). This finding suggests that some types of metal ion are included and play critical roles in the active molecule.

I therefore performed inductively coupled plasma mass spectrometry (ICP-MS) on the purified fraction to measure the contents of metals. 7.5 ppb of Mg, 49.2 ppb of Cu, and

191.3 ppb of Zn were detected in the 20-fold-concentrated purified fraction (Table 1), corresponding to 3.1 μM, 7.8 μM, and 29.0 μM respectively, in the calcium assay systems.

## 4.4. Responsiveness of GPR39-1a against divalent metal ions

In order to determine whether the activity of the purified fraction was due to any of these metals, I tested the activities of $ZnCl_2$, $CuSO_4$, and $MgCl_2$ by calcium mobilization assay with HC48 (Fig. 4a-d). Both $ZnCl_2$ and $CuSO_4$ were found to have concentration-dependent activities specific to HC48, while $MgCl_2$ exhibited no activity in either HC48 or CHO-K1 cells. The potency of $CuSO_4$ for HC48 was not sufficient to explain the activity of the purified fraction, since more than 100 μM Cu (II) ion would be needed to exhibit activity equal to that of the purified fraction. On the other hand, the potency of $ZnCl_2$ for HC48 is consistent with the amount measured in the purified fraction. The activity of the fraction was compared with $ZnCl_2$ activity between 10 and 100 μM. The Zn detected in the purified fraction was found to be equivalent to 29 μM, and within this range. I therefore concluded that the isolated active constituent in this study is $Zn^{2+}$ ion.

## 4.5. Characterization of signaling pathway of GPR39-1a

I then tested the inhibitory effects of pertussis toxin (PTx) and a phospholipase C

(PLC) inhibitor, U73122, to determine whether this activity is mediated through $G_q\alpha$ or $G_i\alpha$. The activity of $ZnCl_2$ was abolished by U73122, while no inhibitory effects were observed with PTx (Fig. 4e). This finding indicates that the calcium-mobilizing activity of $Zn^{2+}$ is mediated through the $G_q\alpha$-PLC pathway.

Finally, I tested $ZnCl_2$ activity with cells transiently expressing mouse and rat GPR39-1a (mGPR39-1a and rGPR39-1a, respectively). Like hGPR39-1a, mGPR39-1a and rGPR39-1a were each also activated by both $ZnCl_2$ and $CuSO_4$ with quick, transient increases in intracellular calcium (Fig. 5a, b). These findings indicate that the function of GPR39-1a as a Zn(II)-sensing receptor is conserved in rodents, as well.

## 5. Discussion

In this chapter, I attempted to find natural agonists of GPR39-1a in FBS, using intracellular calcium mobilization as an index. To accomplish this, I performed two types of HPLC, cation-exchange (CE) and multi-mode (MM), on the peptide fraction conditioned from FBS. The active constituent was isolated, purified, and finally identified as $Zn^{2+}$ by ICP-MS. In addition, I showed that the calcium-mobilizing activity of GPR39-1a is mediated through $G_q\alpha$, using PTx and a PLC inhibitor. I also showed that the function of GPR39-1a as a $Zn^{2+}$-sensing receptor is preserved across species, by assays with mGPR39-1a and rGPR39-1a. In discussing my findings, I consider the following three issues.

The first is that $Zn^{2+}$, the agonist of GPR39-1a, was isolated from peptide fraction of FBS, indicating that it was absorbed by the reverse-phase column in the conditioning phase. Of course, free $Zn^{2+}$ ion itself is not absorbed by reverse-phase columns. $Zn^{2+}$ probably formed complexes with carrier molecules (with molecular weight less than 10KDa) in the reverse-phase step, and dissociated from the carriers at some point in the following steps. Two considerations are suggested by the properties of $Zn^{2+}$: one is the conditions of elution by NaCl gradient in CE, while the other is the starting buffer (pH 9.0, as titrated by NaOH) of MM. In these conditions, sodium ion is present in high concentration, and may replace $Zn^{2+}$ bound to

the carrier molecules.

Second, I found only $Zn^{2+}$ in the peptide fraction of FBS. While I pretreated serum with acetic acid and ethanol followed by ultrafiltration to remove high-molecular-weight proteins, I assume that serious loss of peptides did not occur with this method. Indeed, I found active fractions for angiotensin 1A receptor in a pilot study with the peptide fraction conditioned in the same fashion (data not shown). These findings suggest that there are no peptidergic molecules in FBS to activate GPR39-1a, or that, even if such molecules exist, their concentrations are extremely low.

Third, GPR39-1a functions as a Gq-coupled $Zn^{2+}$-sensing receptor, and this function is conserved across species. Consistent with previous reports (1, 8, 9), I found that $Zn^{2+}$ acts as an agonist at GPR39-1a, inducing quick, transient increase in intracellular calcium. This activity was not abolished by PTx, but was by a PLC inhibitor, indicating that it is mediated through the $G_q\alpha$-PLC pathway. The agonistic activities of $Zn^{2+}$ at GPR39-1a were observed with both mouse and rat GPR39-1a. This finding indicates that the reactivity of GPR39-1a to $Zn^{2+}$ is not limited to humans, but is present in rodents as well. The function of GPR39-1a as a $Zn^{2+}$-sensing receptor is thus likely to be physiologically significant.

Several findings have been reported suggesting the existence of extracellular $Zn^{2+}$-sensing receptors in cells in a variety of tissues (15 - 19). Because the concentrations of

$Zn^{2+}$ ion efficacious for those receptors, reportedly 10-100 μM, are consistent with those for GPR39-1a, it is possible that GPR39-1a corresponds to some of those receptors. The salient question now is that whether the concentrations of $Zn^{2+}$ ion present *in vivo* are sufficient to activate GPR39-1a. In one peripheral organ, the pancreas, about 20 mM of Zn is contained in secretion vesicles of the islets of Langerhans (20), and is released together with insulin (21). In the central nervous system (CNS) , the existence of free zinc ions is observed in synaptic vesicles of the hippocampus and other structures (22, 23). In addition, it has been reported that the concentration of zinc ion sometimes rises to 100-300 μM in synaptic clefts (24, 25). These locally and temporally restricted increases in $Zn^{2+}$ concentrations are sufficient to activate GPR39-1a. In other organs, where no such high concentrations of $Zn^{2+}$ release have been detected, serum is a potential source of $Zn^{2+}$. Indeed, the total content of Zn in FBS is about 30 μM (26), while that in serum of experimental animals and humans is reportedly 10-20 μM (27, 28, 29). Regulation of $Zn^{2+}$ concentration through the bloodstream thus appears to be of importance in modulating the function of GPR39-1a in many peripheral organs.

## 6. Figures and Tables

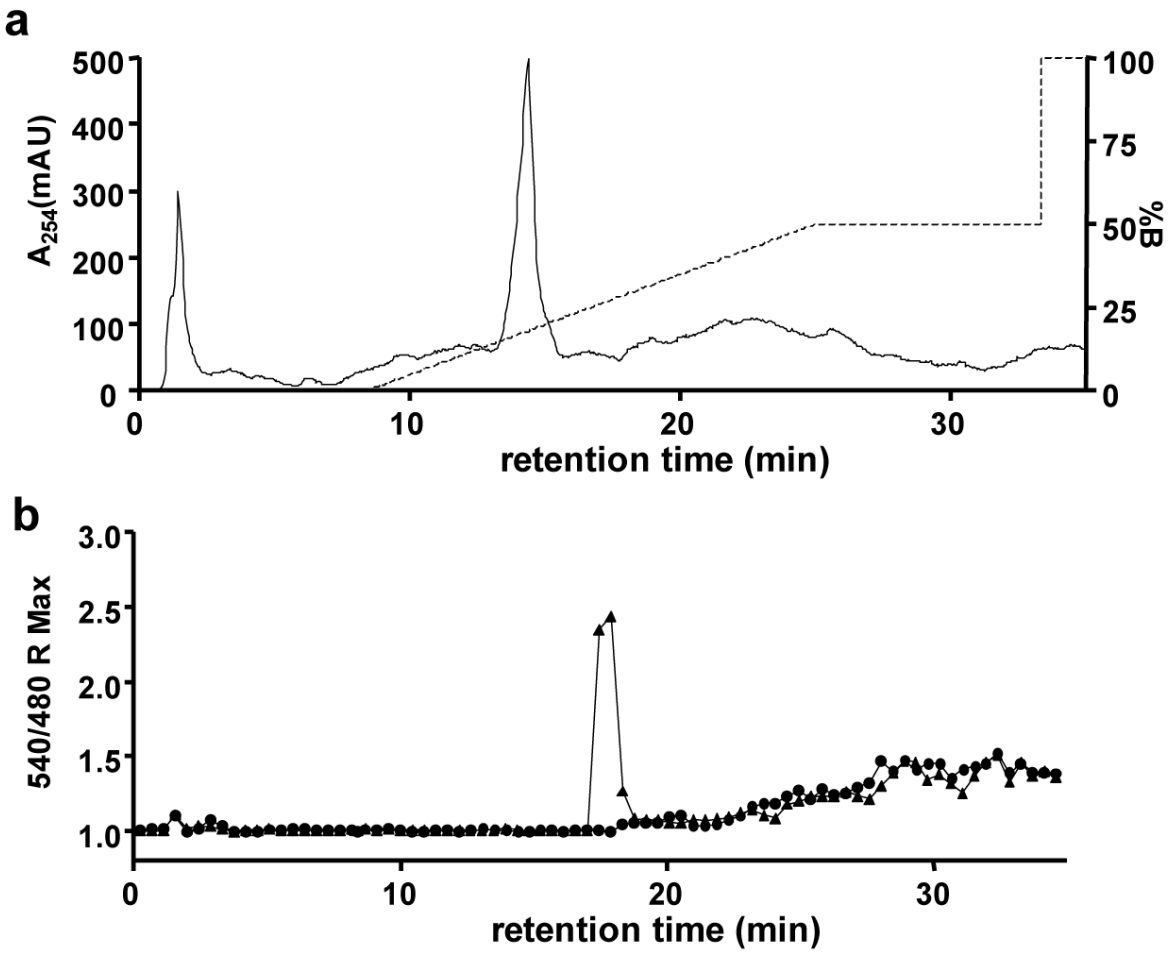


Fig. 2 Fractionation of the peptide fraction of FBS by cation-exchange HPLC**.** a, Cation-exchange HPLC of the peptide fraction conditioned from FBS. The gradient profile is expressed as the mixing ratio of eluent B (*broken line*). Absorbance at 254 nm is indicated by the *solid line*. b, Calcium-mobilizing activity of each fraction assayed with HC48 (▲) and CHO-K1 (●). Tested aliquots were equivalent to 10 mL FBS in assay systems with a total volume of 50 μL. The intensity of each fraction is represented by the maximum fluorescence ratio over the baseline during two minutes of assay time.

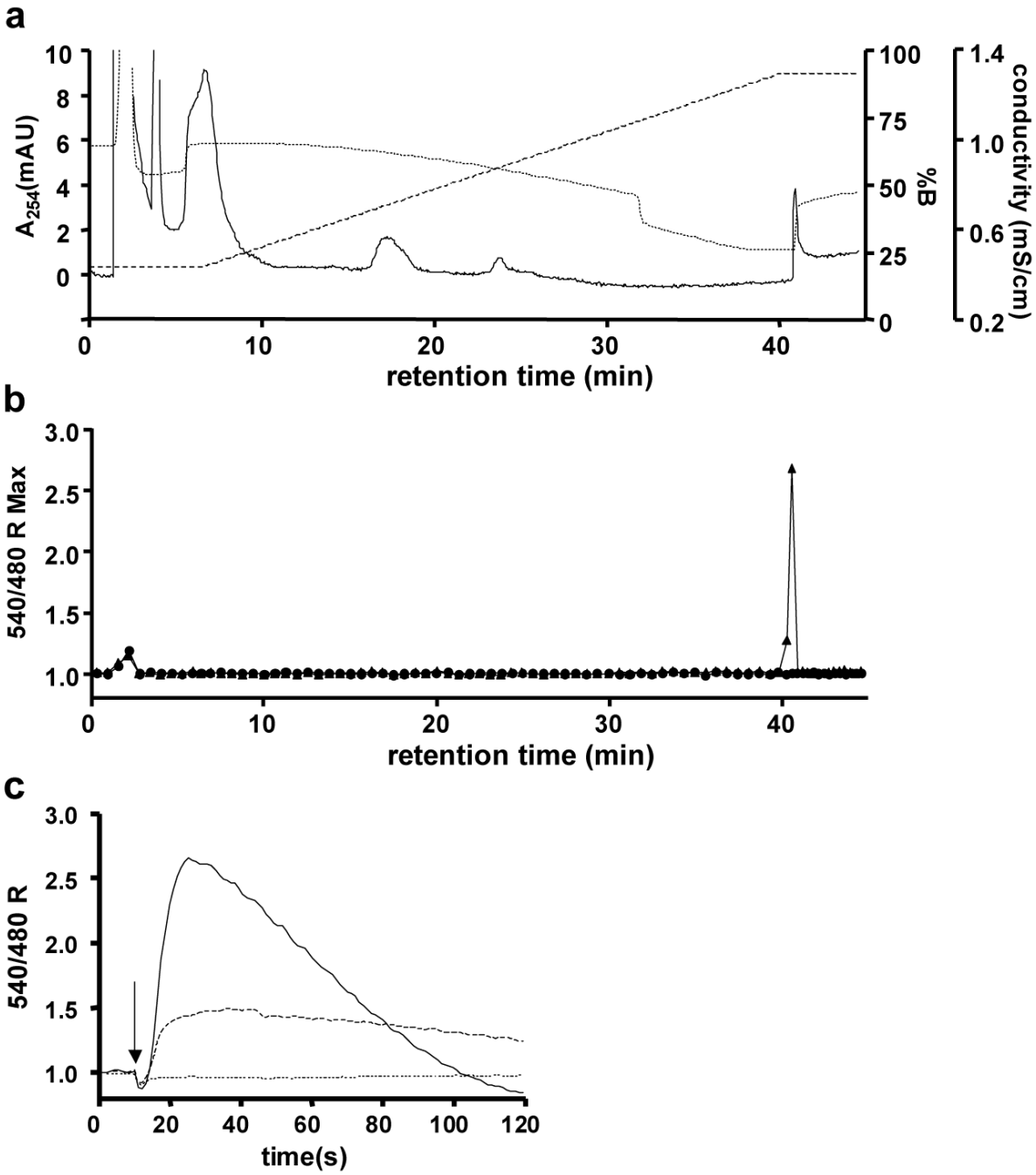


Fig. 3 Purification of the active fractions by multi-mode HPLC. a, Multi-mode HPLC of the active fraction isolated by cation-exchange. The gradient profile is expressed as the mixing ratio of eluent B (*broken line*). Absorbance at 254 nm is indicated by the *solid line*. Electrical conductivity is indicated by the *dotted line*. b, Calcium-mobilizing activity of each fraction assayed with HC48 (▲) and CHO-K1 (●). Tested aliquots were equivalent to 10 mL FBS in assay systems with a total volume of 50 μL. The intensities of each fraction are represented by the maximum fluorescence ratio over the baseline during two minutes of assay time. c, Time course of intracellular calcium mobilization in HC48 cells stimulated by the purified fraction. Activity is expressed as the 540 nm fluorescence ratio

over the baseline with excitation at 480 nm. Total time of measurement is about two minutes. Samples are added to the assay systems at the time point indicated by the *arrow*. The activities of aliquots equivalent to 10 mL FBS, 1 mL FBS, and 10 mL FBS mixed with 300 nM EDTA are indicated by the *solid line*, the *broken line*, and the *dotted line* respectively.

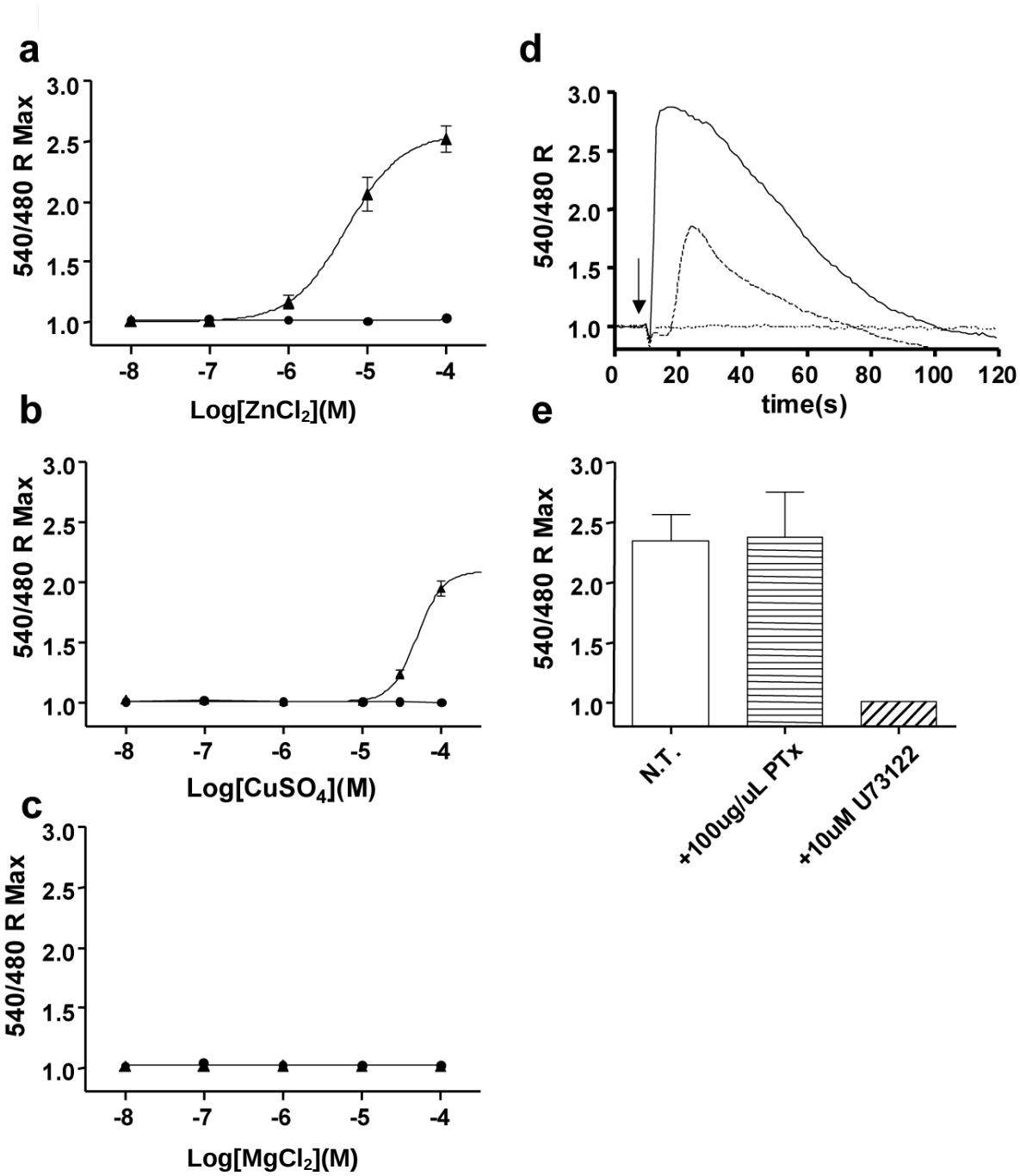


Fig. 4 Calcium-mobilizing activities of Zn, Cu, and Mg ions with HC48. a-c, Dose-response curves for HC48 (▲) and CHO-K1 (●) treated with $ZnCl_2$ (a), $CuSO_4$ (b), and $MgCl_2$ (c). Each of the activities is expressed as the maximum value of the 540 nm fluorescence ratio over the baseline during the two-minute period of measurement. Values are the means and S.E. obtained from 5-6 separate measurements. d, Time course of intracellular calcium mobilization in HC48 cells stimulated by 100 μM of $ZnCl_2$ (*solid line*), $CuSO_4$ (*broken line*), and $MgCl_2$ (*dotted line*). Each of the activities is expressed as the 540 nm fluorescence ratio over the baseline with excitation at 480 nm. Total time of measurement is about two minutes. Samples are added to the assay systems at the time point indicated

by the *arrow*. e, Effects of PTx and U73122 on the activity of $ZnCl_2$. Increases in intracellular calcium concentration of HC48 were measured with stimulation by 100 μM $ZnCl_2$. Cells were pretreated with 100μg/mL PTx or 10μM U73122. PTx was added to the cells on the day before assay, while U73122 was added about ten minutes prior to measurements. Values are the means and S.E. of maximum fluorescence ratio obtained with 5-6 separate measurements.

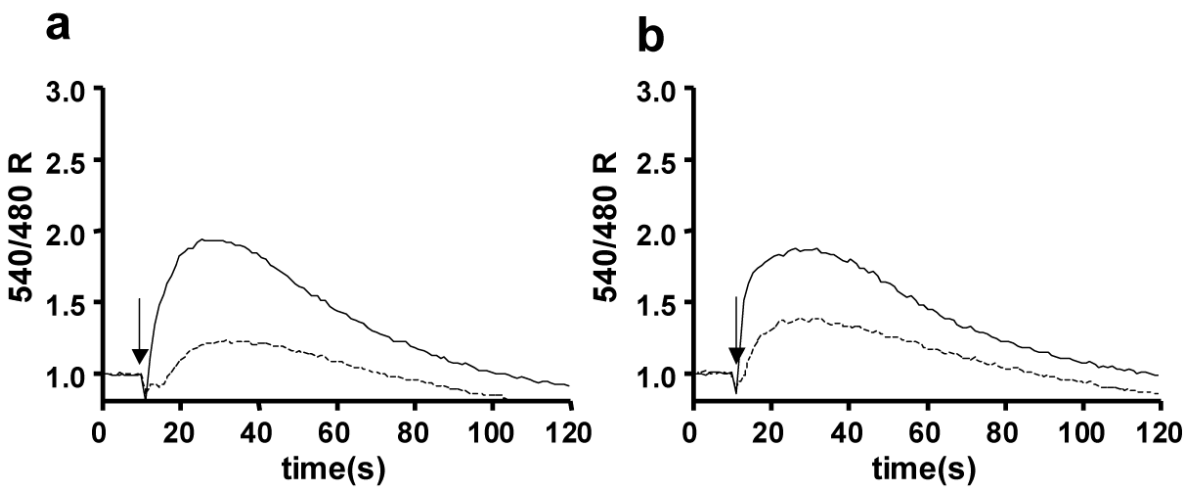


Fig. 5 Preservation of function of GPR39 across species. Time course of intracellular calcium mobilization with CHO-K1 cells transiently expressing mGPR39 (a) or rGPR39 (b) treated with 100μM of $ZnCl_2$ (*solid line*) or $CuSO_4$ (*broken line*). Samples are added to the assay systems at the time point indicated by the *arrows*.

Table 1. Concentration of each metal atom in the purified fraction measured by ICP-MS.

| | atomic mass | measured conc. (ppb) |
|---|---|---|
| Mg | 24.31 | 7.48 ± 0.14 |
| Cr | 52.00 | 0.56 ± 0.00 |
| Fe | 55.85 | 0.00 ± 0.00 |
| Mn | 54.94 | 0.37 ± 0.01 |
| Cu | 63.55 | 49.18 ± 0.43 |
| Zn | 65.39 | 191.31 ± 1.76 |
| Se | 78.96 | 0.00 ± 0.00 |

Measured aliquot was equivalent to 200 mL FBS dissolved in 10 mL solution. Values are means ± S.E. by ten times of measurements.

# CHAPTER Ⅲ. GPR39-1b INTERACTS WITH NEUROTENSIN RECEPTOR NTSR1 AND MODIFIES ITS FUNCTION

## 1. Summary

In this chapter, the molecular functions of GPR39-1b were explored in cell culture. In contrast to GPR39-1a, GPR39-1b showed no response to $Zn^{2+}$ stimulation in calcium mobilization assays, suggesting that GPR39-1b is not a functional receptor of $Zn^{2+}$. To understand the signaling interaction of GPR39-1b, the dimerization between the isoforms was investigated, and bioluminescence resonance energy transfer ($BRET^2$) assays were conducted. The results indicated that GPR39-1b homodimerized, but did not heterodimerize with GPR39-1a. Subsequently, searching the heterodimeric counterparts of GPR39-1b was attempted. Neurotensin receptor 1 (NTSR1) was also targeted as a GPR39-1b interacting partner because of its highly conserved amino acid sequence and mRNA localization, which was similar to GPR39-1b. $BRET^2$ assays demonstrated that GPR39-1b heterodimerized with NTSR1. To examine the effect of GPR39-1b on NTRS1-mediated cAMP/PKA signaling, the cAMP responsive element-luciferase assays was demonstrated, and it was observed that GPR39-1b attenuated neurotensin-induced

NTSR1 signaling. Taken together, the results in this chapter provided a novel regulatory mechanism for GPR39-1b in NTRS1 signaling.

## 2. Introduction

Most of the receptors in the ghrelin receptors family are involved in the regulation of metabolism and nutrition uptake. GHSR is expressed in the brain and stomach and functions as the cognate receptor of ghrelin, an appetite-inducing hormone (2). NTSR1, NTSR2, and GPR38 are expressed in the small intestine and works as the receptors of the hormones controlling intestinal motility and fecal transit, neurotensin (NTS) and motilin (5,30). It is expected that GPR39 also has physiological roles in energy metabolism because *GPR39* null mice showed abnormalities such as obesity (31), altered glucose tolerance (31, 32), pancreatic malfunctions (33-35), and accelerated gastric emptying (36-38).

*GPR39* is known to encode two isoforms, GPR39-1a and -1b (4). GPR39-1a is a full-length 7-transmembrane receptor, which is primarily expressed in the liver, stomach, and pancreas. As shown in the Chapter Ⅱ, GPR39-1a serves as a receptor of $Zn^{2+}$ ion and mobilizes intracellular calcium. According to the reports from another group, the intracellular signaling of GPR39-1a is mediated by cAMP increase and extracellular signal-regulated kinase (ERK) phosphorylation as well (3,40). In the pancreas, it is thought that GPR39-1a is activated to regulate insulin secretion in response to a transient increase in extracellular $Zn^{2+}$. Extracellular $Zn^{2+}$ level elevations are rare in the other

tissues except the brain (24, 25). Considering the broad tissue distribution, GPR39-1a may have biological roles other than $Zn^{2+}$-sensing receptor. On the other hand, GPR39-1b is a truncated 5-transmembrane isoform of GPR39, composed of the extracellular N-terminal and 1st-5th transmembrane domains (TMI-V) (4). GPR39-1b is expressed primarily in the stomach and small intestine, but its molecular function, including $Zn^{2+}$ binding, remains unknown.

GHSR-1b, the 5-transmembrane isoform of GHSR, interacts with the full-length isoform GHSR-1a to attenuate ghrelin-activated signaling (41). In another case, artificially truncated forms of NTSR2 heterodimerize with NTSR1 and inhibit NTS signaling (42). These suggest that direct interaction between GPCRs or its isoforms is physiologically important. However, the physiological significance of GPR39-1b and GPR39-1a or other homologous receptors interactions are unclear. In the present study, the molecular characteristics of GPR39-1b were investigated to understand the regulatory role of GPR39-1b in intracellular signaling by the functional association with GPCRs.

# 3. Materials and Methods

## 3.1. Cloning of genes

Cloning of GPR39-1a was described in the Chapter Ⅱ. GPR39-1b, NTSR1, and GRP109a were cloned using polymerase chain reaction (PCR) from human genomic DNA. For functional assays, expression vectors of these genes were obtained by subcloning them into the pCDNA3.1 vector (Life technologies, Carlsbad, CA). Expression vectors of donor and acceptor for $BRET^2$ assays (43) were obtained by subcloning the GPCR genes into pRluc-N and $pGFP_2$-N protein fusion vectors (Perkin Elmer, Waltham, MA), respectively. The cAMP responsive element-luciferase (CRE-Luc) reporter gene was obtained by subcloning six consecutive CRE sequences, the promoter of the vasoactive intestinal polypeptide (VIP) gene (44), and the luciferase gene into pGL3 vector (Promega Co., Madison, WI). The promoter of VIP was inserted into the position between the 6CREs and the luciferase gene in order to magnify the signal.

## 3.2. Calcium mobilization assays

CHO-K1 cells (American Type Culture Collection) and HC48 cells, a CHO-K1-based cell line stably expressing GPR39-1a already reported in described in the Chapter Ⅱ, were grown in DMEM/F12 (Life technologies) supplemented with 10% fetal

bovine serum (FBS). Cells were harvested with 0.025% Trypsin-EDTA (Life technologies) and loaded with 4 μM Fluo-3AM (Molecular Probes, Inc., Eugene, OR) for 1 h in assay buffer (Hank's balanced salt solution supplemented with 10 mM HEPES, 2.5 mM probenecid, and 0.1% BSA). After loading, cells were washed twice with assay buffer and plated at $2.0 \times 10^4$ cells/well in half-area 96-well clear-bottom black plates (Coring Costar Co., Cambridge, MA). Intracellular calcium ion content was detected by monitoring fluorescence at 540 nm with excitation at 480 nm on a Functional Drug Screening System 6000 (Hamamatsu Photonics KK, Hamamatsu, Japan). For each sample tested, the maximum fluorescence:baseline intensity ratio was calculated over 2 min; this was considered the intensity of calcium response.

## 3.3. CRE-luciferase reporter assays

HEK293 cells (American Type Culture Collection) were grown in DMEM (Life technologies) supplemented with 10% FBS. Cells were transfected with the CRE-Luc reporter gene, described above, together with GPCRs. The following day, cells were harvested by 0.025% trypsin-EDTA (Life technologies), washed once with assay buffer (OPTI-MEM supplemented with 0.1% BSA), and plated at $5 \times 10^4$ cells/well in 96-well white plates (Coring Costar Co., Cambridge, MA). Plates were filled with assay buffer

with NTS at 1, 0.1, and 0.01 μM as the final concentration and incubated for 5 h at 37°C. After the incubation, Steady-Glo (Promega Co.) diluted with lysis buffer (10% SDS-PBS) was added to the cells. Sample luminescence was measured by ARVO-SX (Perkin Elmer).

### 3.4. BRET$^2$ assays

BRET$^2$ (43) was modified from BRET by replacing yellow fluorescence protein (YFP), the acceptor protein, with green fluorescence protein2 ($GFP_2$). The donor vector pRluc-N, containing a GPCR fused to Rluc (*Renilla* luciferase), and the acceptor vector p$GFP_2$-N, containing a GPCR fused to$GFP_2$, were prepared as described above. HEK293 cells were plated at $2 \times 10^4$ cells/well in 96-well collagen coated plate (Corning Costar) 3 days before the assay. The following day, donor (0, 10, 20, 40, 60, 80, and 100 ng/well) and acceptor (50 ng/well) vectors were co-transfected into the HEK293 cells and incubated overnight. At the day of the assay, cells were washed once and filled with 40 μL of assay buffer (D-PBS supplemented with 0.15% glucose, 1 mM $MgCl_2$, 1 mM $CaCl_2$, and 2 μg/mL of aprotinin). After 10 μL of 25 μmol/L DeepBlueC (Perkin Elmer) was added, the fluorescence intensity at 410 nm and 515 nm were measured to determine the activity of Rluc and the signal caused by BRET$^2$, respectively. The 515 nm fluorescence raised by 405 nm laser was also measured by ARVO light (Perkin Elmer) to determine the

basal level of $GFP_2$ fluorescence. The $BRET^2$ signal was calculated by the equation below.

$BRET^2$ signal = (Emission at 515 nm - Emission at 515 nm of non-transfected cells)

/ (Emission at 410 nm - Emission at 410 nm of non-transfected cells)

# 4. Results

## 4.1. Calcium mobilization assays in the cells transfected with GPR39-1b

Calcium mobilization assays were performed to determine if GPR39-1b alone acts as a $Zn^{2+}$ receptor. In HC48 cells, a CHO-K1-based cell line stably expressing GPR39-1a, $ZnCl_2$ induced the mobilization of intracellular calcium (Fig. 6a, square). In contrast, GPR39-1b transfected CHO-K1 cells did not mobilize intracellular calcium in response to $ZnCl_2$ (Fig. 6b, triangle) compared with that in non-transfected cells (Fig. 1b, square). This result indicated that GPR39-1b is not a functional receptor for $Zn^{2+}$. To investigate the effect of GPR39-1b on GPR39-1a signaling, HC48 cells were transfected with GPR39-1b and stimulated with $ZnCl_2$. GPR39-1b transfection did not affect the $ZnCl_2$-induced intracellular calcium mobilization mediated by GPR39-1a (Fig. 6a, triangle).

## 4.2. $BRET^2$ assays to evaluate the homodimerization and heterodimerization across the isoforms of GPR39 gene

$BRET^2$ assays were carried out to evaluate the physical interactions between GPR39 isoforms. Various amounts of GPR39-1a-$GFP_2$ vector were co-transfected into

HEK293 cells along with the GPR39-1b-Rluc vector, and the fluorescence signal was measured after the addition of the Rluc substrate. $BRET^2$ was not observed between GPR39-1a-$GFP_2$ and GPR39-1b-Rluc (Fig. 7a). However, under identical condition, GPR39-1b-$GFP_2$ and GPR39-1b-Rluc showed $BRET^2$ (Fig. 7b). These results indicated that GPR39-1b homodimerized, but did not heterodimerize with GPR39-1a.

## 4.3. $BRET^2$ assays to explore the heterodimeric counterpart of GPR39-1b

It was assumed that GPR39-1b exerted its functions by interacting with other GPCRs, and the heterodimeric counterparts of GPR39-1b was explored using the $BRET^2$ system. Heterodimerization tends to occur between structurally homologous receptors (45), and receptor co-localization is an important physiological factor with regard to their physical interactions. NTSR1 is a member of the ghrelin receptor family and structurally homologous to GPR39-1b (3). Moreover, similar to GPR39-1b, NTSR1 is expressed in the brain and small intestine (4, 46). GPR109a, a class A orphan GPCR is expressed in the colon and small intestine (47), like as GPR39-1b. Thus, NTSR1 and GPR109a were chosen as candidate GPR39-1b heterodimerization partners. NTSR1 and GPR109a were fused with Rluc to construct the donor vector for the $BRET^2$ system and co-transfected

into HEK293 cells with various amounts of the acceptor vector GPR39-1b-$GFP_2$. As shown in Fig. 3a, $BRET^2$ between NTSR1-Rluc and GPR39-1b-$GFP_2$ exhibited a saturation curve that depended on the $GPF_2$:Rluc ratio with a non-linear equation. This result indicated that GPR39-1b heterodimerized with NTSR1. The interaction of these receptors was confirmed by swapping donor and acceptor (Fig. 8c). On the other hand, co-transfection with GPR109-Rluc and GPR39-1b-$GFP_2$ did not result in a $BRET^2$ signal (Fig. 8b), indicating no interaction.

## 4.4. CRE-Luc assays to evaluate the functional effects of heterodimerization on the signaling activity of NTSR1

It is presumed that cAMP signaling is important for the NTSR1-mediated regulation of $Cl^-$ secretion by the small intestine. Therefore, I focused on NTSR1-mediated cAMP signaling. The functional role of GPR39-1b:NTSR1 heterodimerization in NTSR1 signaling was examined using CRE-Luc reporter gene assays. CRE-Luc, NTSR1, and varying amounts of GPR39-1b vectors were transfected into HEK293 cells. As shown in Fig. 9, the NTS-triggered luminescence signal was attenuated depending on the amounts of GPR39-1b transfected. This result indicated that GPR39-1b and NTSR1 heterodimerization inhibited NTSR1-mediated cAMP/PKA signaling. To confirm that NTSR1 expression levels were not altered, fluorescence was measured in HEK293 cells co-transfected with NTSR1-$GFP_2$ and GPR39-1b. The fluorescence intensity evoked from NTSR1-$GFP_2$ was not affected by the amount of GPR39-1b transfected, indicating that GPR39-1b did not interfere with NTSR1 expression (Fig. 10).

## 5. Discussion

Recently, truncated isoforms of some GPCRs have been identified (41, 48, 49). However, their functions of most of them are still unclear. In this study, the molecular function of one of such molecules, GPR39-1b was explored.

GPR39-1b contains an extracellular $Zn^{2+}$ binding domain, but lacks the intracellular domains that interact with heterotrimeric G proteins (40). Therefore, it is assumed that GPR39-1b does not have functions to transduce extracellular signals into the cells even if it can bind to $Zn^{2+}$ ions. In this study, calcium mobilization assays demonstrated that GPR39-1b was nonresponsive to $ZnCl_2$. $BRET^2$ assay demonstrated that GPR39-1b homodimerized, but did not heterodimerize with GPR39-1a. In addition, it was confirmed that GPR39-1b did not modulate the calcium mobilizing activity of GPR39-1a. This is not the case of GHSR-1b, a short isoform of the GHSR gene translation product. GHSR-1b heterodimerizes with and modifies the signaling activity of GHSR-1a, a full-length isoform (41).

It was hypothesized that GPR39-1b works by heterodimerizing with other GPCRs similar in amino acid sequence and tissue distribution. The results indicated that NTSR1, the NTS receptor, heterodimerized with GPR39-1b. In particular, CRE-Luc reporter gene assays showed that GPR39-1b suppressed the NTSR1-mediated

cAMP/PKA-signaling pathway. NTSR1 signaling interference was previously reported for NTSR2, a subtype of NTSR1 (42). NTSR2 regions important for the attenuation of NTSR1 signaling are identified to be TM I-IV because the strongest suppression was shown by the NTSR2 mutants lacking TM V-VII and the C-terminal intracellular domain. Because GPR39 shares sequence similarities with NTSR2, the GPR39-1b-associated inhibition of NTSR1 signaling may have a similar mechanism.

NTSR1 couples to both $G_q$ and $G_s$ to increase intracellular calcium and cAMP, respectively (30). The $G_s$/cAMP signal is involved in $Cl^-$ release from the epithelium of the small intestine and colon (50, 51) where NTS treatment evokes $Cl^-$ secretion and accelerates fecal transit in the gastrointestinal tract (52, 53). As described above, NTSR2 inhibit NTSR1 signaling (42), but NTSR2 is mostly expressed in the brain (54). Therefore, NTSR2 is unlikely involved in the regulation of intestinal $Cl^-$ secretion and fecal transit. Considering that GPR39-1b repressed NTSR1 signaling, GPR39-1b may prevent $Cl^-$ secretion and delay fecal transit. Interestingly, it is reported that *GPR39* null mice, lacking both GPR39-1a and GPR39-1b, exhibit accelerated fecal transit (36). This is consistent if GPR39-1b constitutively suppresses the NTSR1 signaling that promotes fecal excretion (55) and the loss of GRP39-1b increase defecation. *GPR39* null mice also exhibit increased gastric emptying (36). This phenotype cannot be explained by

GPR39-1b inhibition of NTSR1 signaling because NTSR1 slows gastric emptying (56).

In conclusion, the findings in this chapter highlighted a novel regulatory function of GPR39-1b in NTSR1 signaling. Recent reports showed that the brain GPR39-1b mRNA levels are greater than GPR39-1a mRNA levels (4), and the injection of antisense GPR39-1b into the rat brain induces anxiety (57). In any case, the molecular and physiological effects of GPR39-1b-mediated inhibition of NTSR1 signaling in the gastrointestinal tract, brain, and the other tissues still remain unrevealed. Further characterization is necessary in order to fully understand the physiological significance of GPR39-1b.

## 6. Figures and Tables

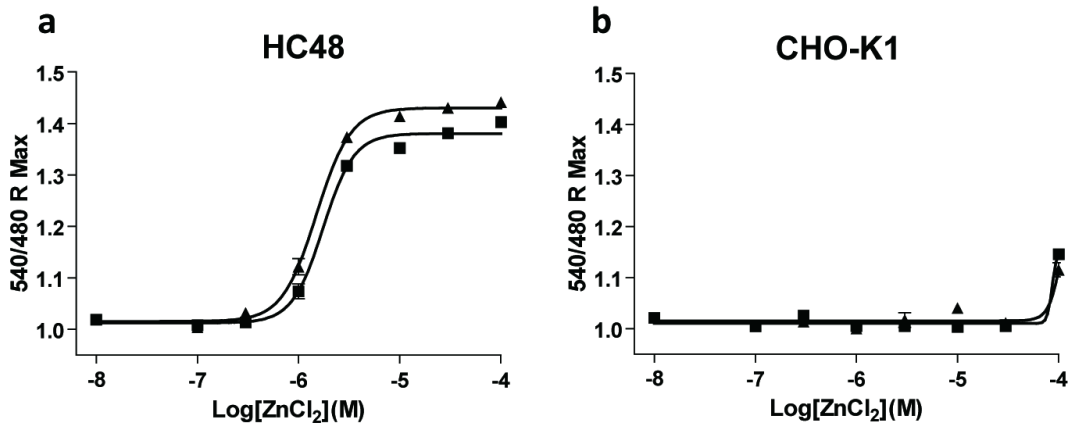


Fig. 6 Calcium-mobilizing activities of $Zn^{2+}$ in cells transfected with GPR39-1b**.** Dose-response curves for HC48 (a) and CHO-K1 (b) cells treated with $ZnCl_2$. Cells were transfected with GPR39-1b (▲) or control vector (■). Activities are expressed as the maximum value of the 540 nm fluorescence ratio over baseline during a 2-min measurement. Values are means ± standard error (SE) obtained from four individual measurements.

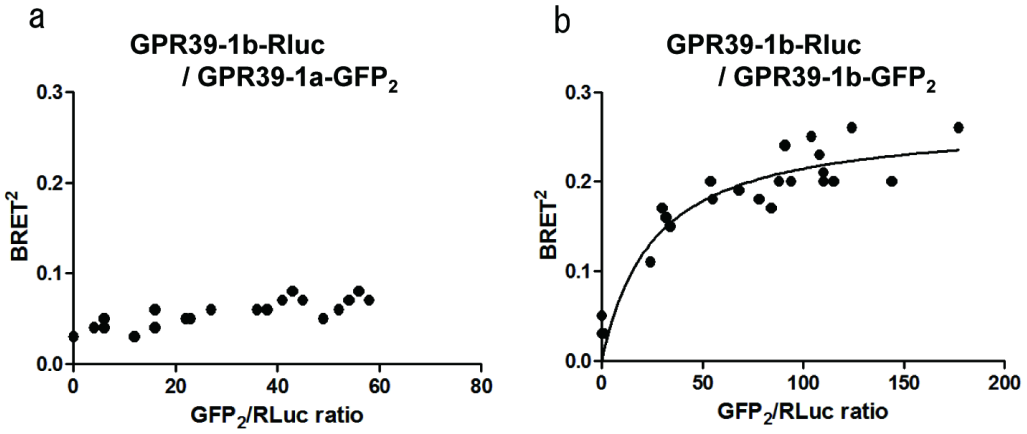


Fig. 7 $BRET^2$ assays of GPR39 isoforms.

GPR39-1b-Rluc was co-transfected into HEK293 cells with GPR39-1a-$GFP_2$ (a) or GPR39-1b-$GFP_2$ (b). Total luminescence and fluorescence were measured. $BRET^2$ values were not increased according to the $GFP_2$/Rluc ratio. The nonlinear regression equation did not converge, suggesting that GPR39-1a and GPR39-1b did not interact (a). For cells transfected with GPR39-1b-Rluc and GPR39-1b-$GFP_2$, a saturation curve was obtained with a nonlinear regression equation that assumed a single binding site where $R^2 = 0.88$ (b).

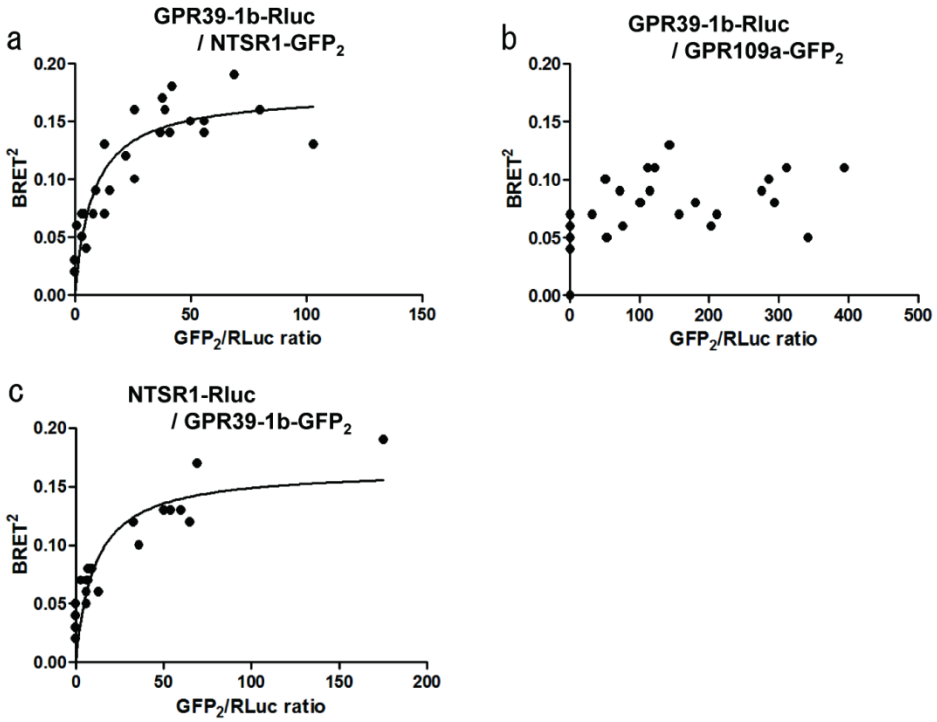


Fig. 8 $BRET^2$ assays of GPR39-1b with NTSR1 and GPR109a.

GPR39-1b-Rluc was co-transfected into HEK293 cells with NTSR1-$GFP_2$ (a) and GPR109a-$GFP_2$ (b). Total luminescence and fluorescence were measured. For GPR39-1b-Rluc and NTSR1-$GFP_2$, a saturation curve was obtained with nonlinear regression equation ($R^2$ = 0.77). To confirm heterodimerization, the donor and acceptor were swapped. NTSR1-Rluc was co-transfected into HEK293 cells with GPR39-1b-$GFP_2$ (c). A saturation curve was obtained with a nonlinear regression equation ($R^2$ = 0.62).

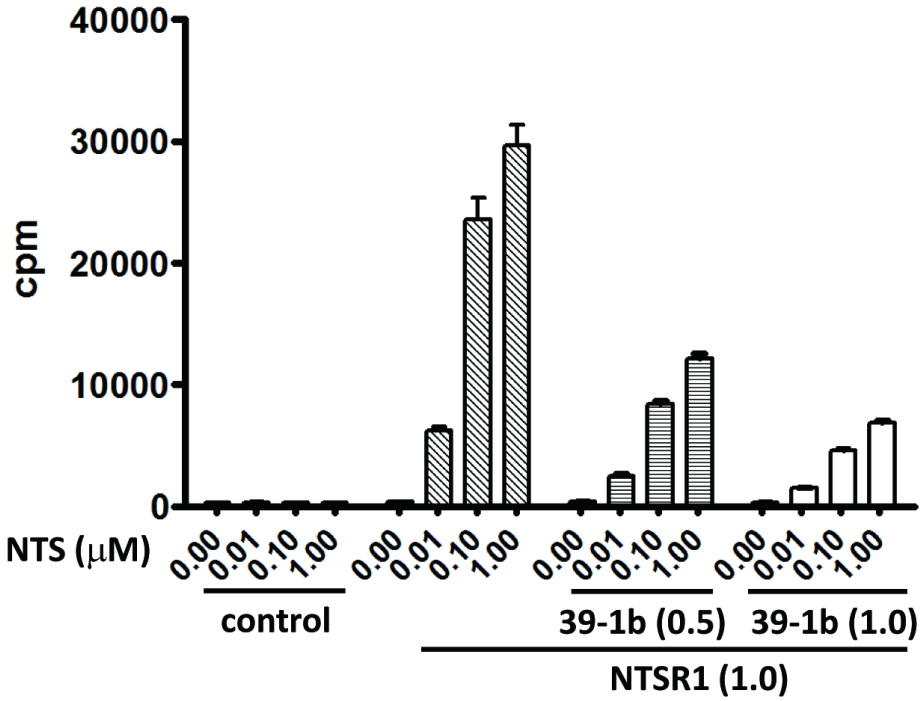


Fig. 9 Effects of GPR39-1b and NTSR1 co-expression on the NTS-CRE signal.
GPR39-1b was transiently co-expressed with NTRS1 and the CRE-Luciferase reporter gene in HEK293 cells. Control are cells transfected with the CRE-Luc and empty vector. The amounts of DNA transfected are indicated in parentheses (μg/2 × $10^6$ cells). Each of the NTS-induced luciferase activities is expressed as luminescence. Values are means ±SE obtained from three individual measurements.

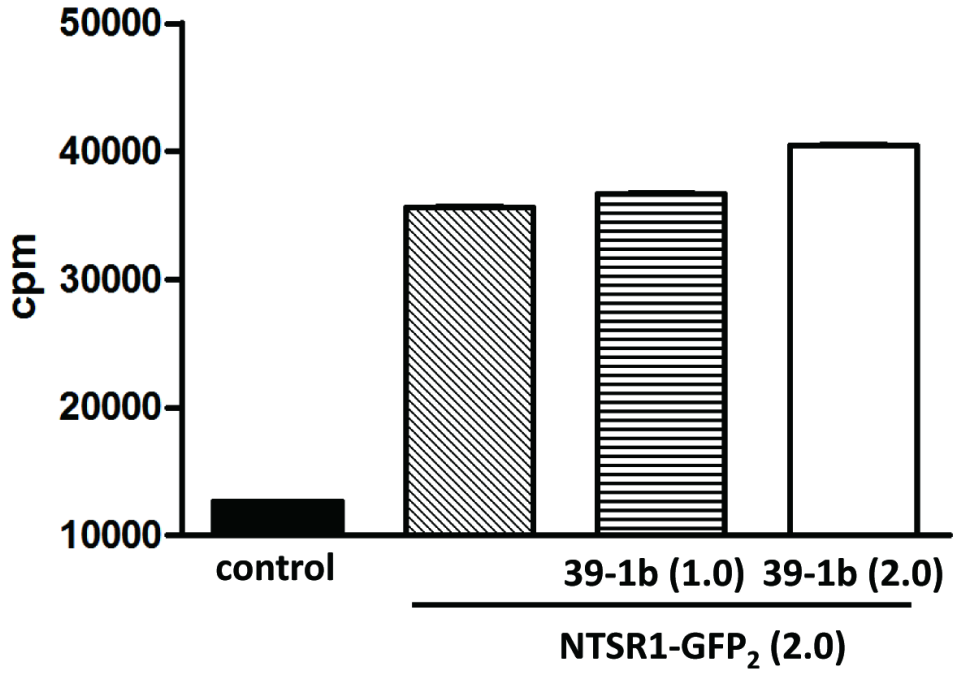


Fig. 10 Effects of co-expression of GPR39-1b on NTSR1 gene transcription.
GPR39-1b was transiently co-expressed in HEK293 cells with NTSR1-$GFP_2$. Control are cells transfected with empty vector. The amounts of DNA transfected are indicated in the parentheses (μg/6 × $10^6$ cells). Each of the activities is expressed as fluorescence. Values are means ± SE obtained from 16 separate measurements.

# CHAPTER Ⅳ. CONCLUDING REMARKS

In the present study, the molecular functions of two isoforms, GPR39-1a and GPR39-1b, encoded in the GPR39 gene, were characterized.

In the Chapter Ⅱ, GPR39-1a, the full-length 7-transmembrane isoform, whose ligands and functions had been unknown, was revealed as a $G_q$-coupled $Zn^{2+}$-sensing receptor. It is known that $Zn^{2+}$ ion has many bioactivities in the body, while their mechanisms are unclear. On the other hand, the physiological importance of GPR39 gene is being elucidated by genetically engineered models in several institutes. The findings of the present study may give a link between bioactivities of $Zn^{2+}$ ion and the physiological roles of the GPR39 gene.

In the Chapter Ⅲ, a new molecular function of GPR39-1b, the truncated isoform, was discovered. GPR39-1b heterodimerized with NTSR1, a receptor of neurotensin, and inhibited its signaling activity. This means GPR39-1b may have a role to modulate the activity of neurotensin and to work as a regulator of gastrointestinal transit. This finding may explain one aspect of the physiological meaning of GPR39-1b in the GI tract. Moreover, this finding can shed light on the importance of the molecular functions of short isoforms of GPCRs.

As described above, the present study newly elucidated molecular functions of the two isoforms of GPR39, GPR39-1a and GPR39-1b. These findings are expected to provide clues for

further understanding on the physiological roles of the GPR39 gene.

# CHAPTER Ⅴ. ACKNOWLEDGEMENTS

I would like to express my deep gratitude to all those who provided me guidance, support and encouragement during the preparation of this dissertation.

Most of all, I would like to express my sincere thanks to Professor Akiyoshi Fukamizu and Dr. Junji Ishida for valuable guidance and encouragement in this study.

I also would like express my gratitude to Takahiro Miyazaki, Masami Yamashita, Kouji Munechika, Akihito Kamizono, and Dr. Yoshitaka Ikeda for their helpful guidance and valuable discussion.

I also thank Yasufumi Fukano, Kazuhiro Yano, Noriko Matsunaga, Nahoko Maruyama, Motonori Hashimoto, Taro Kishimoto, Minoru Obata, Dr. Emiko Sugikawa, Dr. Mitsuhiro Kikyo, Moeko Kanai, and Fumiko Yamairi for technical instruction and assistance.

I am deeply indebted Dr. Kenji Arakawa, Dr. Yutaka Ito, and Dr. Masaaki Nagasaki for encouraging and supporting this work.

# CHAPTER Ⅵ. REFERENCES


1. Rask-Andersen M, Almén MS, Schiöth HB. Trends in the exploitation of novel drug targets. Nat Rev Drug Discov (2011),10(8),579-90.
2. Kojima M, Hosoda H, Date Y, Nakazato M, Matsuo H, Kangawa K. Ghrelin is a growth-hormone-releasing acylated peptide from stomach. Nature (1999),402,656-660.
3. Holst B, Holliday ND, Bach A, Elling CE, Cox HM, Schwartz TW. Common structural basis for constitutive activity of the ghrelin receptor family. J Biol Chem (2004),279,53806-53817.
4. Egerod KL, Holst B, Petersen PS, Hansen JB, Mulder J, Hökfelt T, Schwartz TW. GPR39 splice variants versus antisense gene LYPD1: expression and regulation in gastrointestinal tract, endocrine pancreas, liver, and white adipose tissue. Mol Endocrinol (2007),21(7),1685-98..
5. McKee KK, Tan CP, Palyha OC, Liu J, Feighner SD, Hreniuk DL, Smith RG, Howard AD, Van der Ploeg LH. Cloning and characterization of two human G protein-coupled receptor genes (GPR38 and GPR39) related to the growth hormone secretagogue and neurotensin receptors. Genomics (1997),46,426-434.
6. Zhang JV, Ren PG, Avsian-Kretchmer O, Luo CW, Rauch R, Klein C, Hsueh AJ.

Obestatin, a peptide encoded by the ghrelin gene, opposes ghrelin's effects on food intake. Science (2005),310,996-999.

7. Jackson, VR, Nothacker HP, Civelli O. GPR39 receptor expression in the mouse brain. Neuroreport (2006),17,813-816.

8. Holst B, Egerod KL, Schild E, Vickers SP, Cheetham S, Gerlach LO, Storjohann L, Stidsen CE, Jones R, Beck-Sickinger AG, Schwartz TW. GPR39 signaling is stimulated by zinc ions but not by obestatin. Endocrinology (2007),148,13-20.

9. Lauwers E, Landuyt B, Arckens L, Schoofs L, Luyten W. Obestatin does not activate orphan G protein-coupled receptor GPR39. Biochem Biophys Res Commun (2006),351,21-5.

10. Chartrel N, Alvear-Perez R, Leprince J, Iturrioz X, Reaux-Le Goazigo A, Audinot V, Chomarat P, Coge F, Nosjean O, Rodriguez M, Galizzi JP, Boutin JA, Vaudry H, Llorens-Cortes C. Comment on "Obestatin, a peptide encoded by the ghrelin gene, opposes ghrelin's effects on food intake". Science (2007),315,766.

11. Gourcerol G, St-Pierre DH, Tache Y. Lack of obestatin effects on food intake: Should obestatin be renamed ghrelin-associated peptide (GAP)? Regul Pept (2007),141,1-7.

12. Minamino N, Tanaka J, Kuwahara H, Kihara T, Satomi Y, Matsubae M, Takao T. Determination of endogenous peptides in the porcine brain: possible construction of

peptidome, a fact database for endogenous peptides. J Chromatogr B Analyt Technol Biomed Life Sci (2003),792,33-48.

13. Cohn EJ. Demonstration of new processes of blood collection and separation of red blood cells, white blood cells, and platelets; protein glycoprotein, lipoprotein, and other components of plasma. Science (1950),112,450-451.

14. Stevenson BJ, Hagenbuchle O, Wellauer PK. Sequence organisation and transcriptional regulation of the mouse elastase II and trypsin genes. Nucleic Acids Res (1986),14,8307-8330.

15. Sharir H, Hershfinkel M. The extracellular zinc-sensing receptor mediates intercellular communication by inducing ATP release. Biochem Biophys Res Commun (2005),332,845-852.

16. Azriel-Tamir H, Sharir H, Schwartz B, Hershfinkel M. Extracellular zinc triggers ERK-dependent activation of Na+/H+ exchange in colonocytes mediated by the zinc-sensing receptor J Biol Chem (2004),279,51804-51816.

17. Park KS, Lee NG, Lee KH, Seo JT, Choi KY. The ERK pathway involves positive and negative regulations of HT-29 colorectal cancer cell growth by extracellular zinc Am J Physiol Gastrointest Liver Physiol (2003),285,G1181-G1188.

18. McNulty TJ, Taylor CW. Extracellular heavy-metal ions stimulate Ca2+ mobilization in

hepatocytes. Biochem J (1999),339,555-561.

19. Zsembery A, Fortenberry JA, Liang L, Bebok Z, Tucker TA, Boyce AT, Braunstein GM, Welty E, Bell PD, Sorscher EJ, Clancy JP, Schwiebert EM. Extracellular zinc and ATP restore chloride secretion across cystic fibrosis airway epithelia by triggering calcium entry. J Biol Chem (2004),279,10720-10729.

20. Hutton JC, Penn EJ, Peshavaria M. Low-molecular-weight constituents of isolated insulin-secretory granules. Bivalent cations, adenine nucleotides and inorganic phosphate. Biochem J (1983),210,297-305.

21. Figlewicz DP, Forhan SE, Hodgson AT, Grodsky GM. 65Zinc and endogenous zinc content and distribution in islets in relationship to insulin content. Endcrinology (1984),115,877-881.

22. Frederickson CJ, Danscher G. Zinc-containing neurons in hippocampus and related CNS structures. Prog Brain Res (1990),83,71-84.

23. Brown CE, Dyck RH. Distribution of zincergic neurons in the mouse forebrain. J Comp Neurol (2004),479,156-167.

24. Assaf SY, Chung SH. Release of endogenous Zn2+ from brain tissue during activity. Nature (1984),308,734-736.

25. Howell GA, Welch MG, Frederickson CJ. Stimulation-induced uptake and release of zinc

in hippocampal slices. Nature (1984),308,736-738.

26. Data sheets provided by Hyclone.

27. Lowe NM, Bremner I, Jackson MJ. Plasma 65Zn kinetics in the rat. Br J Nutr (1991),65,445-455.

28. Folin M, Contiero E, Vaselli GM. Zinc content of normal human serum and its correlation with some hematic parameters. Biometals (1994),7,75-79.

29. Bideci A, Camurdan MO, Cinaz P, Dursun H, Demirel F. Serum zinc, insulin-like growth factor-I and insulin-like growth factor binding protein-3 levels in children with type 1 diabetes mellitus. J Pediatr Endocrinol Metab (2005),18,1007-1011.

30. Vincent JP, Mazella J, Kitabgi P. Neurotensin and neurotensin receptors. Trends Pharmacol Sci (1999),20,302-309.

31. Petersen PS, Jin C, Madsen AN, Rasmussen M, Kuhre R, Egerod KL, Nielsen LB, Schwartz TW, Holst B. Deficiency of the GPR39 receptor is associated with obesity and altered adipocyte metabolism. FASEB J (2011),25(11),3803-14.

32. Verhulst PJ, Lintermans A, Janssen S, Loeckx D, Himmelreich U, Buyse J, Tack J, Depoortere I. GPR39, a receptor of the ghrelin receptor family, plays a role in the regulation of glucose homeostasis in a mouse model of early onset diet-induced obesity. J Neuroendocrinol (2011),23(6),490-500.

33. Egerod KL, Jin C, Petersen PS, Wierup N, Sundler F, Holst B, Schwartz TW. β-Cell Specific Overexpression of GPR39 Protects against Streptozotocin-Induced Hyperglycemia. Int J Endocrinol (2011),2011,401258.

34. Tremblay F, Richard AM, Will S, Syed J, Stedman N, Perreault M, Gimeno RE. Disruption of G protein-coupled receptor 39 impairs insulin secretion in vivo. Endocrinology (2009),150(6),2586-95.

35. Holst B, Egerod KL, Jin C, Petersen PS, Østergaard MV, Hald J, Sprinkel AM, Størling J, Mandrup-Poulsen T, Holst JJ, Thams P, Orskov C, Wierup N, Sundler F, Madsen OD, Schwartz TW. G protein-coupled receptor 39 deficiency is associated with pancreatic islet dysfunction. Endocrinology (2009),150(6),2577-85.

36. Moechars D, Depoortere I, Moreaux B, de Smet B, Goris I, Hoskens L, Daneels G, Kass S, Ver Donck L, Peeters T, Coulie B. Altered gastrointestinal and metabolic function in the GPR39-obestatin receptor-knockout mouse. Gastroenterology (2006),131(4),1131-41.

37. Depoortere I. GI functions of GPR39: novel biology. Curr Opin Pharmacol (2012),12(6),647-52.

38. Popovics P, Stewart AJ. GPR39: a Zn(2+)-activated G protein-coupled receptor that regulates pancreatic, gastrointestinal and neuronal functions. Cell Mol Life Sci (2011),68(1),85-95.

39. Holst B, Egerod KL, Schild E, Vickers SP, Cheetham S, Gerlach LO, Storjohann L, Stidsen CE, Jones R, Beck-Sickinger AG, Schwartz TW. GPR39 signaling is stimulated by zinc ions but not by obestatin. Endocrinology (2007),148(1),13-20.

40. Storjohann L, Holst B, Schwartz TW. Molecular mechanism of Zn2+ agonism in the extracellular domain of GPR39. FEBS Lett (2008),582(17),2583-8.

41. Mary S, Fehrentz JA, Damian M, Gaibelet G, Orcel H, Verdié P, Mouillac B, Martinez J, Marie J, Banères JL. Heterodimerization with Its splice variant blocks the ghrelin receptor 1a in a non-signaling conformation: a study with a purified heterodimer assembled into lipid discs. J Biol Chem (2013), 288(34), 24656-65..

42. Hwang JR, Baek MW, Sim J, Choi HS, Han JM, Kim YL, Hwang JI, Kwon HB, Beaudet N, Sarret P, Seong JY. Intermolecular cross-talk between NTR1 and NTR2 neurotensin receptor promotes intracellular sequestration and functional inhibition of NTR1 receptors. Biochem Biophys Res Commun (2010),391(1),1007-13.

43. Jensen AA, Hansen JL, Sheikh SP, Bräuner-Osborne H. Probing intermolecular protein-protein interactions in the calcium-sensing receptor homodimer using bioluminescence resonance energy transfer (BRET). Eur J Biochem (2002),269(20),5076-87.

44. Fitzgerald LR, Mannan IJ, Dytko GM, Wu HL, Nambi P. Measurement of Responses

from Gi-, Gs-, or Gq-Coupled Receptors by a Multiple Response Element/cAMP Response Element-Directed Reporter Assay. Anal Biochem (1999),275(1),54-61.

45. Levoye A, Dam J, Ayoub MA, Guillaume JL, Jockers R. Do orphan G-protein-coupled receptors have ligand-independent functions? New insights from receptor heterodimers. EMBO Rep (2006),7(11),1094-8.

46. Tanaka K, Masu M, Nakanishi S. Structure and functional expression of the cloned rat neurotensin receptor. Neuron (1990),4(6),847-54.

47. Thangaraju M, Cresci GA, Liu K, Ananth S, Gnanaprakasam JP, Browning DD, Mellinger JD, Smith SB, Digby GJ, Lambert NA, Prasad PD, Ganapathy V. GPR109A is a G-protein-coupled receptor for the bacterial fermentation product butyrate and functions as a tumor suppressor in colon. Cancer Res (2009), 69(7), 2826-32.

48. Bagher AM, Laprairie RB, Kelly ME, Denovan-Wright EM. Co-expression of the human cannabinoid receptor coding region splice variants (hCB1) affects the function of hCB1 receptor complexes. Eur J Pharmacol (2013),721(1-3),341-54.

49. Watson SJ, Brown AJ, Holliday ND. Differential signaling by splice variants of the human free fatty acid receptor GPR120. Mol Pharmacol (2012),81(5),631-42.

50. Field M, Sheerin HE, Henderson A, Smith PL. Catecholamine effects on cyclic AMP

levels and ion secretion in rabbit ileal mucosa. Am J Physiol (1975),229(1),86-92.

51. Brown DR, Treder BG. Neurohormonal regulation of ion transport in the porcine distal jejunum. Actions of neurotensin and its natural homologs. J Pharmacol Exp Ther (1989),249(1),348-57.

52. Mandel KG, Dharmsathaphorn K, McRoberts JA. Characterization of a cyclic AMP-activated Cl-transport pathway in the apical membrane of a human colonic epithelial cell line. J Biol Chem (1986),261(2),704-12.

53. Riegler M, Castagliuolo I, Wang C, Wlk M, Sogukoglu T, Wenzl E, Matthews JB, Pothoulakis C. Neurotensin stimulates Cl(-) secretion in human colonic mucosa In vitro: role of adenosine. Gastroenterology (2000),119(2),348-57.

54. Chalon P, Vita N, Kaghad M, Guillemot M, Bonnin J, Delpech B, Le Fur G, Ferrara P, Caput D. Molecular cloning of a levocabastine-sensitive neurotensin binding site. FEBS Lett (1996),386(2-3),91-4.

55. Calam J, Unwin R, Peart WS. Neurotensin stimulates defaecation. Lancet (1983),1(8327),737-8.

56. Blackburn AM, Fletcher DR, Bloom SR, Christofides ND, Long RG, Fitzpatrick ML, Baron JH. Effect of neurotensin on gastric function in man. Lancet (1980),1(8176),987-9.

57. Ishitobi Y, Akiyoshi J, Honda S, Ninomiya T, Kanehisa M, Tanaka Y, Tsuru J, Isogawa

K, Kitamura H, Fujikura Y. Administration of antisense DNA for GPR39-1b causes anxiolytic-like responses and appetite loss in rats. Neurosci Res (2011),72(3),257-62.